Biochemistry

Article

Discovery of an irreversible and cell-active BCL6 inhibitor selectively targeting Cys53 located at the protein-protein interaction interface

Tomoya Sameshima, Takeshi Yamamoto, Osamu Sano, Satoshi Sogabe, Shigeru Igaki, Kotaro Sakamoto, Koh Ida, Mika Gotou, Yasuhiro Imaeda, Junichi Sakamoto, and Ikuo Miyahisa

Biochemistry, **Just Accepted Manuscript** • DOI: 10.1021/acs.biochem.7b00732 • Publication Date (Web): 02 Jan 2018

Just Accepted

ACS Publications

Biochemistry is published by the American Chemical Society. 1155 Sixteenth Street N.W., Washington, DC 20036

Discovery of an irreversible and cell-active BCL6 inhibitor selectively targeting Cys53 located at the protein–protein interaction interface

Tomoya Sameshima[*†], Takeshi Yamamoto[*], Osamu Sano, Satoshi Sogabe, Shigeru Igaki, Kotaro Sakamoto[§], Koh Ida, Mika Gotou, Yasuhiro Imaeda, Junichi Sakamoto and Ikuo Miyahisa[†]

Pharmaceutical Research Division, Takeda Pharmaceutical Company Limited, 26-1, Muraoka-higashi 2 chome, Fujisawa, Kanagawa, Japan.

* These authors equally contributed to this work

[†]*Corresponding authors:*

Tomoya Sameshima, Pharmaceutical Research Division, Takeda Pharmaceutical Company Limited, 26-1, Muraoka-Higashi 2-chome, Fujisawa, Kanagawa, Japan.

E-mail: tomoya.sameshima@takeda.com

Ikuo Miyahisa: Pharmaceutical Research Division, Takeda Pharmaceutical Company Limited, 26-1, Muraoka-Higashi 2-chome, Fujisawa, Kanagawa, Japan.,

E-mail: ikuo.miyahisa@takeda.com

Keywords: irreversible inhibitor, B-cell lymphoma 6 (BCL6), protein–protein interaction, irreversible fluorescent probe

ABSTRACT:

B-cell lymphoma 6 (BCL6) is the most frequently involved oncogene in diffuse large B-cell lymphomas (DLBCLs). BCL6 shows potent transcriptional repressor activity through interactions with its corepressors, such as BCL6 corepressor (BCOR). The inhibition of the protein–protein interaction (PPI) between BCL6 and its corepressors suppresses the growth of BCL6-dependent DLBCLs, thus making BCL6 an attractive drug target for lymphoma treatments. However, potent small-molecule PPI inhibitor identification remains challenging because of the lack of deep cavities at PPI interfaces. This paper reports the discovery of a potent, cell-active, small-molecule BCL6 inhibitor, **BCL6-i** (**8**), that operates through irreversible inhibition. First, we synthesized an irreversible lead compound **4**, which targets Cys53 in a cavity on the BCL6 BTB domain dimer by introducing an irreversible warhead to a high-throughput screening hit compound **1**. Further chemical optimization of **4** based on k_{inact}/K_I evaluation produced **BCL6-i** with a k_{inact}/K_I value of 1.9×10^4 $M^{-1}s^{-1}$, corresponding to a 670-fold improvement in potency compared to **4**. By exploiting the property of irreversible inhibition, engagement of **BCL6-i** to intracellular BCL6 was confirmed. **BCL6-i** showed intracellular PPI inhibitory activity between BCL6 and its corepressors, thus resulting in BCL6-dependent DLBCL cell-growth inhibition. **BCL6-i** is a cell-active chemical probe with the most potent BCL6 inhibitory activity reported to date. The discovery process of **BCL6-i** illustrates the utility of irreversible inhibition for

identifying potent chemical probes for intractable target proteins.

■ Introduction

B-cell lymphoma 6 (BCL6), a member of the bric-à-brac, tramtrack and broad complex/ poxvirus and zinc finger (BTB/POZ) family of transcription factors,[1, 2] is the most frequently involved oncogene in diffuse large B-cell lymphoma (DLBCL).[3, 4] BCL6 shows potent transcriptional repressor activity by recruiting corepressors, such as silencing mediator for retinoid and thyroid receptors (SMRT),[5, 6] nuclear receptor corepressor (NCOR),[6] and BCL6 corepressor (BCOR),[7] to an exposed surface groove formed at the interface of the two chains in the BTB dimer (Figure 1).[8, 9] Because inhibition of the protein–protein interaction (PPI) between BCL6 and its corepressor by peptide inhibitors represses DLBCL cell growth,[10–12] BCL6 is considered to play an essential role in lymphoma-cell survival, thus making it a promising therapeutic target for lymphoma treatments.[11, 13] However, small-molecule PPI inhibitor identification remains challenging despite great efforts in academia and pharmaceutical industries. A major obstacle for identifying small-molecule PPI inhibitors is the lack of deep cavities for binding small molecules in PPI interfaces;[14–17] therefore, larger molecules are required to achieve potent PPI inhibition compared to other target classes. In fact, ligand efficiency of known PPI inhibitors is generally smaller than those of the inhibitors for other target classes, such as protein kinase and protease.[17]

Therefore, BCL6 inhibitor identification with small molecular weight is considered challenging. To date, some small-molecule BCL6 inhibitors have been reported, but they lack potency (K_i = 10–100 μM),[18, 19] and their utility as a chemical probe is potentially limited.

Targeted covalent inhibition has emerged as an efficient strategy for potent-inhibitor identification. Targeted covalent inhibition shows potent efficacy owing to their prolonged interaction with their target proteins,[20–23] thus, they have been applied to many drug-discovery projects,[24] e.g. kinase inhibitors.[22, 25, 26] In fact, approximately one-third of all enzyme targets whose FDA-approved inhibitor exists have an example of an approved covalent drug.[21] Specifically, irreversible covalent inhibitors are expected to exert excellent efficacy because release from inhibition requires re-synthesis of the target protein. Therefore, we hypothesized that exploiting irreversible inhibition could be a powerful strategy for potent small-molecule PPI inhibitor identification. Despite this advantage, irreversible inhibitors have long been avoided in many drug-discovery programs because of their potential to promiscuously modify off-target proteins, leading to adverse effects such as immunotoxicity or hypersensitivity.[27-29] To avoid such adverse effects, irreversible inhibitors with low intrinsic chemical reactivity need to be designed. This study describes a strategy for identifying the potent, cell-active, small-molecule BCL6 inhibitor **BCL6-i** (**8**) by exploiting irreversible inhibition with acceptable intrinsic chemical reactivity for *in vivo* testing. **BCL6-i** shows the most potent BCL6 inhibitory activity among all small-molecule BCL6 inhibitors

reported thus far.[18, 19] The discovery of **BCL6-i** illustrates the utility of irreversible inhibition for identifying potent chemical probes for intractable target classes, including PPI. Herein, we also demonstrate the research process for cell-active irreversible inhibitor identification using an irreversible fluorescent ligand.

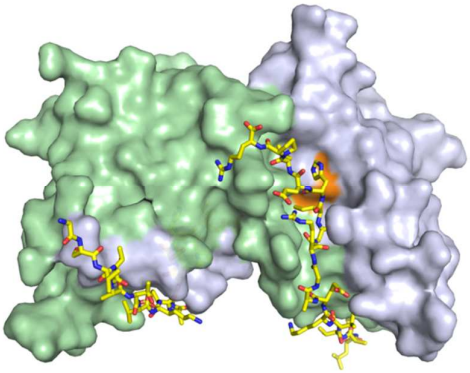

Figure 1. Crystal structure of the BCL6 BTB domain in a complex with its corepressor SMRT (PDB code, 1R2B).[9] The two BTB dimer chains are shown in green and blue, and the two SMRT peptides are shown in stick representation with yellow carbon atoms. Cys53 in the cavity of BCL6 is highlighted in orange.

■ MATERIALS AND METHODS

Materials

Sodium chloride, magnesium acetate, acetonitrile, trifluoroacetic acid (TFA), adenosine triphosphate (ATP), and d-biotin were purchased from Wako (Osaka, Japan). Bicine buffer was obtained from MP biomedicals (Santa Ana, CA). Solutions of 4-(2-hydroxyethyl)-1-piperazineethanesulfonic acid (HEPES), DMEM (Dulbecco's Modified Eagle's Medium), phosphate buffered saline (PBS), and RPMI1640 medium (containing

HEPES) were purchased from Thermo Fisher Scientific (Waltham, MA). Fetal bovine serum (FBS) was obtained from Corning (Corning, NY). Terbium-labeled streptavidin (Tb-SA) was purchased from Cisbio (Codolet, France). The detergent 3-[(3-cholamidopropyl)-dimethylammonio] propanesulfonate (CHAPS) was obtained from Dojindo (Kumamoto, Japan). Tween-20 was purchased from Bio-Rad (Hercules, CA). CI-1033[30, 31] was purchased from Haoyuan Chemexpress (Shanghai, China). WZ8040[32] was obtained from Selleck Chemicals (Houston, TX). All peptides used herein were synthesized in Toray Research Center (Tokyo, Japan). Biotin ligase (BirA) protein was prepared as described previously.[33]

Preparation of recombinant BCL6 (5–129)

All His-Avi-SUMO-FLAG-BCL6-BTB proteins (5–129) were prepared as described previously.[34] Herein, all BCL6-BTB proteins contained C8Q, C67R, and C84N mutations. To biotinylate the BCL6-BTB (C53/C121) protein, 30 μM Avi-SUMO-BCL6-BTB protein was incubated with 0.12 μM BirA protein in a reaction buffer (50 mM bicine buffer, pH 8.3, 10 mM ATP, 10 mM $Mg(OAc)_2$, and 50 μM d-biotin) at 30 °C for 1 h and BCL6 protein was purified using a HiPrep 26/10 desalting column (GE Healthcare Bio-Sciences, Piscataway, NJ). The other His-Avi-SUMO-FLAG-BCL6-BTB mutant proteins (C53S/C121, C53/C121S, and C53S/C121S) were biotinylated with endogenous biotin ligase in the expression cell (*E.*

coli BL21(DE3) (Nippon Gene, Tokyo, Japan)). To remove the His-Avi-SUMO tag from the BCL6-BTB (C53/C121) protein, the SUMO tag was digested using ubiquitin-like-specific protease 1 (ULP1) (LifeSensors, Malvern, PA) and purified BCL6 protein using Ni-NTA (Qiagen, Hilden, Germany) and Mono Q (GE Healthcare Bio-Sciences) columns, sequentially. The purified protein was stored at −80 °C until use.

Evaluation of covalent modification by protein mass spectrometry (protein-MS)

SUMO tag removed BCL6-BTB (C53/C121) protein (0.2 mg/mL) and 100 μM F1324 peptide (Ac-LWYTDIRMSWRVP-OH) or DMSO were mixed in PBS and incubated for 30 min at room temperature. Subsequently, equal volumes of the test compounds (40 μM) in PBS were added to the sample and incubated at room temperature for 3 h (except for **BCL6-NC**) or 15 h (for **BCL6-NC**). The final concentration of BCL6 protein, test compound, and F1324 were 0.1 mg/mL, 20 μM, and 50 μM, respectively. The reaction was stopped by the addition of equal volumes of 0.2% TFA (final concentration is 0.1%), and the sample was stored at −80 °C until mass spectrometry analysis. Mass spectrometry analysis was performed with a Xevo G2-S TOF (Waters, Milford, MA) equipped with an ESI source. The reverse-phase separation of an intact sample was performed with an Acquity UPLC (Waters) system. Separations were achieved with an Acquity UPLC BEH300 C4 Column (Waters, 2.1 × 50 mm) using acetonitrile:water (both containing 0.025% TFA) as the eluent in a gradient

from 0:10 to 10:0 in 6 min at a 0.6-mL/min flow rate. Mass spectra were acquired in the positive ion mode. The capillary and cone voltages were set at 3,000 and 150 V, respectively. The m/z scan range was set to 400–2500. Deconvolution of the intact sample's ESI mass spectra was performed by BiopharmaLynx 1.3 (Waters) and MassLynx 4.1 (Waters) programs using the MaxEnt 1 algorithm (Waters).

Time-resolved fluorescence resonance energy transfer (TR-FRET) assay

TR-FRET assays were performed using 384-well, white, flat-bottomed plates (product # 784075, Greiner Bio-One, Frickenhausen, Germany). TR-FRET was measured using an EnVision microplate reader (Perkin Elmer, Waltham, MA) with a 320 nm / 75 nm - UV (TRF320) dug11 filter (Perkin Elmer, for excitation), a 590/8 nm photometric filter (Perkin Elmer, for tetramethylrhodamine (TAMRA) emission), a 535 nm/25 nm FITC filter (Perkin Elmer, for Tb emission), and a D400 optical module (Perkin Elmer). All assays were performed with BCL6 assay buffers (25 mM HEPES, 100 mM NaCl, 0.01% (w/v) Tween-20). Throughout this study, Tb-SA and biotinylated BCL6-BTB protein were preincubated in BCL6 assay buffer over 60 min at room temperature before addition to the assay plates.

Measurement of inhibitory activity for the interaction between BCL6 and a reversible-binding peptide

TAMRA-peptide (TAMRA-Abu(4)-VWYTDIRMRDWM) was designed from the F1325 peptide.[34] Several concentrations of test inhibitors in DMSO (50 nL) were dispensed to each well in the assay plate using the Access Echo555 liquid handler. The plate was stored at −30 °C until use. After returning the plate to room temperature, BCL6 assay buffer containing TAMRA-peptide (2.5 μL) was dispensed into each well. Next, the Tb-SA/BCL6-BTB premix was added to the assay solution and incubated at room temperature. The TR-FRET signal was measured using an EnVision plate reader. The final concentrations of Tb-SA, BCL6-BTB, and TAMRA-peptide for each of the BCL6 mutants were as follows; 0.17, 0.50, and 30 nM (C53/C121); 0.17, 8, 90 nM (C53S/C121); 0.17, 8, 70 nM (C53/C121S); 0.17, 16, and 230 nM (C53S/C121S). The fraction of BCL6-BTB complexed to the test compounds was calculated according to equation (1).

$$\text{Inhibition (\%)} = 100 \times \left(\frac{\mu_{C1} - T}{\mu_{C1} - \mu_{C2}} \right) \quad (1)$$

Where T is the value of the wells containing test compounds and μ_{c1} and μ_{c2} are the mean values of the 0% and 100% inhibition control wells, respectively. The values of the 0% and 100% controls were the signals obtained in the presence and absence of BCL6-BTB protein, respectively. Inhibitory activity of test compounds was calculated by fitting the data using a logarithmic equation. Data analysis was performed with the GraphPad Prism 5 program (GraphPad Software, Inc., La Jolla, CA).

Determination of k_{inact}/K_I values for BCL6-FP

The reaction was initiated by the addition of Tb-SA/BCL6-BTB (C53/C121) premix (5 μL) to BCL6 buffer (5 μL) containing various concentrations of **BCL6-FP**. The final concentrations of Tb-SA and BCL6-BTB (C53/C121) were 0.17 and 0.25 nM, respectively. The plate was sealed with MicroAmp® Optical Adhesive Film (Thermo Fisher Scientific, Waltham, MA) to avoid evaporation and the signal was measured with an EnVision plate reader every 5 min. During the time-course measurement, the assay-plate temperature was maintained at 25 °C and the top seal was maintained at 2 °C higher than the assay plate to avoid condensation on the seal. The reaction-specific TR-FRET signal was obtained by subtracting the TR-FRET signal in the absence of BCL6-BTB (C53/C121) from the signal in the presence of BCL6-BTB (C53/C121). The signal was fitted to a single exponential curve (equation (2)) using the GraphPad Prism 5 program.

$$\text{Signal} = (Y_\infty - Y_0)[1 - \exp(-k_{\text{obs}}t)] + Y_0 \qquad (2)$$

,where Y_0, Y_∞ and k_{obs} represent signal at initial and finite time and observed kinetic rate constant, respectively. The k_{obs} values were plotted against the concentration of **BCL6-FP** and the $k_{\text{inact}}/K_{\text{I}}$ value was obtained by fitting the data using equation (3).

$$k_{\text{obs}} = (k_{\text{inact}} / K_{\text{I}})_{\text{probe}}[\mathbf{BCL6\text{-}FP}] \qquad (3)$$

Measurement of k_{inact}/K_I values for test compounds using an irreversible probe

competition (IPC) assay

Several concentrations of test inhibitors in DMSO (50 nL) were dispensed in the assay plate using an Access Echo555 liquid handler (Labsite, Sunnyvale, CA). The plate was stored at −30 °C until use. After returning the plate to room temperature, 2.5 μL of assay buffer containing **BCL6-FP** was dispensed into each well and the plate was shaken for several seconds. Subsequently, equal volumes of Tb-BCL6-BTB (C53/C121) premix was added to the assay solution and incubated at room temperature. The final concentrations of Tb-SA, BCL6-BTB (C53/C121), and **BCL6-FP** were 0.17, 0.25, and 250 nM, respectively. The plate was sealed and the TR-FRET signal was measured using EnVision after a 4 h incubation at room temperature. The fraction of BCL6-BTB (C53/C121) that reacted with the test compounds was calculated according to equation (1). The values of the 0% and 100% controls were the signals obtained in the presence and absence of BCL6-BTB (C53/C121), respectively. The inhibitory activity of test compounds was calculated by fitting the data using a logarithmic equation. Data analysis was performed with the GraphPad Prism 5 program. The IC_{50} value obtained from the assay was converted to a k_{inact}/K_I using equation (4).[35, 36]

$$(k_{\text{inact}} / K_{\text{I}})_{\text{inhibitor}} = \frac{(k_{\text{inact}} / K_{\text{I}})_{\text{probe}}[\text{P}]}{\text{IC}_{50}} \quad (4)$$

, where [P] is the concentration of **BCL6-FP**.

Measurement of intrinsic chemical reactivity using HPLC

Test compound (10 μM) and GSH (1 mM) were mixed into the assay buffer (25 mM HEPES, 1 mM EDTA, 0.5% (w/v) CHAPS) and an aliquot (10 μL) was injected in an Acquity UPLC (Waters Corp., Milford, MA) or Shimadzu UFLC (Shimadzu, Kyoto, Japan) at arbitrary times. The sample was separated by a Unison UK-18 2.0 mm internal diameter × 20 or 30 mm (3 μm) column (Imtakt, Kyoto, Japan) using a gradient elution method: Mobile phase A (distilled water/50 mM ammonium acetate/acetonitrile 8:1:1 (v/v/v)). Mobile phase B (50 mM ammonium acetate/acetonitrile 1:9 (v/v)). Linear gradient from 95 to 40% A in B over 1.5 min; 40% A in B was held for 0.3 min; linear gradient from 40% to 95% A in B over 0.01 min. The flow rate was set at 0.5 mL/min and the column oven was maintained at 50 °C. The elute was monitored with an online UV spectrophotometer (PDA 210-400 nm) and the amount of test compound was determined from the peak area. The percent of test compound remaining was plotted against injection time. k_{chem} was calculated by fitting the data to equation (5) using the GraphPad Prism 5 software.

$$\text{Percentage of remaining} = 100\{1 - \exp(-k_{\mathrm{chem}}[\mathrm{GSH}]t)\} \quad (5)$$

To rule out the possibility of GSH-independent compound decomposition in aqueous solution, decrease in test compounds in the absence of GSH was simultaneously measured (data not shown).

Fluorescence imaging

The FLAG-BCL6 (wild type, full length) plasmid was transfected to U2OS cells using the FuGENE HD transfection reagent (Promega, Madison, WI). The transfected cells were seeded at 3×10^3 cells/25 μL/well on clear bottom 384-well plates (TC-treated CellCarrier-384 Ultra, ref# 6057308, PerkinElmer) in McCoy's medium (Thermo Fisher Scientific) containing 10% FBS. After incubation for 1 h at 37 °C/5% CO_2, medium (10 μL) containing **BCL6-i** or **BCL6-NC** (1 μM final concentration) was added to the plate and further incubated for 1 h at 37 °C/5% CO_2. Subsequently, 10 μL of the medium containing **BCL6-FP** (1 μM final concentration) was added to each well and incubated for 1 h at room temperature. Cells were fixed by adding 15 μL of 16% paraformaldehyde (Wako, final concentration was 4%) in PBS directly into the medium and further incubated for 10 min at room temperature. After removing the medium, the cells were washed with PBS (50 μL). For cell permeabilization and prevention of nonspecific antibody binding, PBS containing 10% goat serum (Thermo Fisher Scientific) and 0.1% Triton-X100 (Wako) was added to each well and incubated for 1 h at room temperature. After removing the medium and washing the cells with PBS (50 μL), the cells were incubated with the FlagM2 antibody (1:1000 dilution) (Sigma-Aldrich, St. Louis, MO) in PBS containing 10% goat serum and 0.1% Triton-X100, followed by incubation overnight at 4 °C. After removing the medium, the cells were washed

with PBS (50 μL) and FLAG-BCL6 was stained using PBS containing the Alexa488-conjugated anti-mouse IgG antibody (Thermo Fisher Scientific) (1:1000 dilution). After removing the medium and washing the cells with PBS, fluorescence images were obtained using an INCell analyzer 6000 (GE Healthcare Bio-Sciences) with a x40 objective lens. The images were analyzed using Image J software (National Institute of Health, MD).

Mammalian two-hybrid assay

The vectors, pGL4.35, pBind, and pACT, were obtained from Promega. As template DNA, human BCL6 cDNA was isolated by PCR from a human skeletal muscle cDNA library (TAKARA Bio, Shiga, Japan) and human BCOR cDNA was purchased from GeneCopoeia Inc. (Rockville, MD). Each cDNA fragment was granted restriction site by PCR and was digested with restriction enzymes to insert into pBIND or pACT, respectively. Mammalian two-hybrid assay (M2H) was performed in HEK293T cells that were transfected with reporter constructs: pGL4.35 containing the GAL4 special response element of firefly luciferase (9xGAL4UAS), pBIND/GAL4-BCL6 (Ala5–Glu129), and pACT/VP16-BcoR(Leu112–Ala753) by FuGENE HD (Promega). The transfected cells were seeded at 1×10^4 cells/15 μL/well on 384-well plates (ref# 3570, Corning, NY, USA) in DMEM containing 10% FBS. After incubation for 24 h with test compounds at 37 °C/5% CO_2, cells were lysed to measure luciferase activity using the Bright-Glo luciferase assay

system (Promega).

Growth inhibition assay

SUDHL4 and OCI-LY3 cells were cultivated in RPMI1640 medium (containing HEPES) containing 10% and 20% FBS, respectively. The cells were seeded at 2500 cells/25 μL/well on 384-well plates (ref# 3570, Corning) and incubated for 24 h at 37 °C/5% CO_2. Subsequently, 10 μL of the medium (containing **BCL6-i** or **BCL6-NC**) was added to the plate and incubated at 37 °C/5% CO_2. The final concentration of inhibitors was 3 μM. After 3 days of incubation, 30 μL of the Cell Titer Glo (Promega) reagent was added to each well and the luminescence was measured using a plate reader. The values of the 0% and 100% controls were obtained from wells containing DMSO treated cells and the medium only, respectively.

■ RESULTS

Identification of 4 as an irreversible BCL6 inhibitor

Through a high-throughput screening of approximately 130,000 compounds, using an enzyme-linked immunosorbent assay that monitored the interaction between the BCL6 protein and its cofactor BCOR peptide, **1** was identified as a BCL6 inhibitor (Figure 2A).[37] Co-crystal structure analysis of **1** showed that it is associated in the BCL6 cavity (Figure 2B). As shown in Figure 2B, Cys53 is located near the binding site of **1**. This Cys53 motivated us

to design and synthesize **2**–**4**, which introduces a chloroacetamide moiety as an irreversible warhead for **1** (Figure 2A). The BCL6 BTB domain (Ala5–Glu129) contains five cysteine residues (Figure S1). Three of the protein residues were substituted with other amino acids (C8Q, C67R, C84N) for higher protein expression and solubility.[9, 19, 34] We analyzed the covalent modification of BCL6-BTB (C53/C121) with **2**–**4** after a 3-h incubation using protein mass spectrometry (protein-MS) analysis (Figure 2C). The results indicated 1:1 stoichiometric covalent modification for **3** (C3–linker) and **4** (C4–linker), and no modification for **2** (C2–linker). Judging from the peak height, the labeling efficiency of **4** was higher than that of **3** (Figure 2C). The difference in the covalent-modification efficiency can be derived from the distance between Cys53 and the chloroacetamide group. It should be noted that the MS peak height may be affected by other factors, such as ionization efficiency of the respective protein. To further support this result, we evaluated the inhibitory activity of these compounds on interactions between the BCL6 protein and its partner peptide. As a reversible fluorescent peptide, a tetramethylrhodamin (TAMRA)-conjugated BCL6 binding peptide (TAMRA-peptide) was prepared, in reference to a previous report,[34] and the interaction was measured using TR-FRET. After 4 h of incubation, the inhibitory activity of **4** was more potent than that of **3** (Figure S2); and **2** did not show inhibitory activity at the concentration of 6.3 μM. The TR-FRET assay result reflected the labeling efficiency observed using protein-MS. According to these results, **4** was selected as the lead compound

for further evaluation.

To investigate the specific covalent modification of Cys53 in BCL6 using **4**, protein-MS analysis was performed in the presence of F1324, a potent BCL6 binding peptide that covers the Cys53-containing cavity in the BCL6-BTB protein.[34] Modification of BCL6-BTB (C53/C121) by **4** was not identified in the presence of F1324, indicating that access to the cavity was blocked by the peptide F1324 (Figure S3). This result suggests that **4** specifically modifies the Cys53 of BCL6.

Next, the irreversibility of **4** to BCL6 was confirmed by a jump dilution assay. Compound **2** (100 μM, 81% inhibition, Figure S4A) and **4** (6.3 μM, 67% inhibition, Figure S4B) were incubated for 10 h with BCL6-BTB (C53/C121), followed by a 100-fold dilution to the buffer containing 20-fold K_d of TAMRA-peptide. After dilution, covalent inhibition by **4** did not change for 24 h (Figure S4C, *red*), whereas non covalent inhibition by **2** rapidly disappeared (Figure S4C, *black*), suggesting irreversible binding of **4** to BCL6-BTB (C53/C121). Conversely, **10**–**12**, which contain acrylamide as the warhead, did not show any BCL6 modification (Figure S5). This result indicated that an appropriate warhead needs to be selected to achieve irreversible covalent modification of the targeted cysteine.

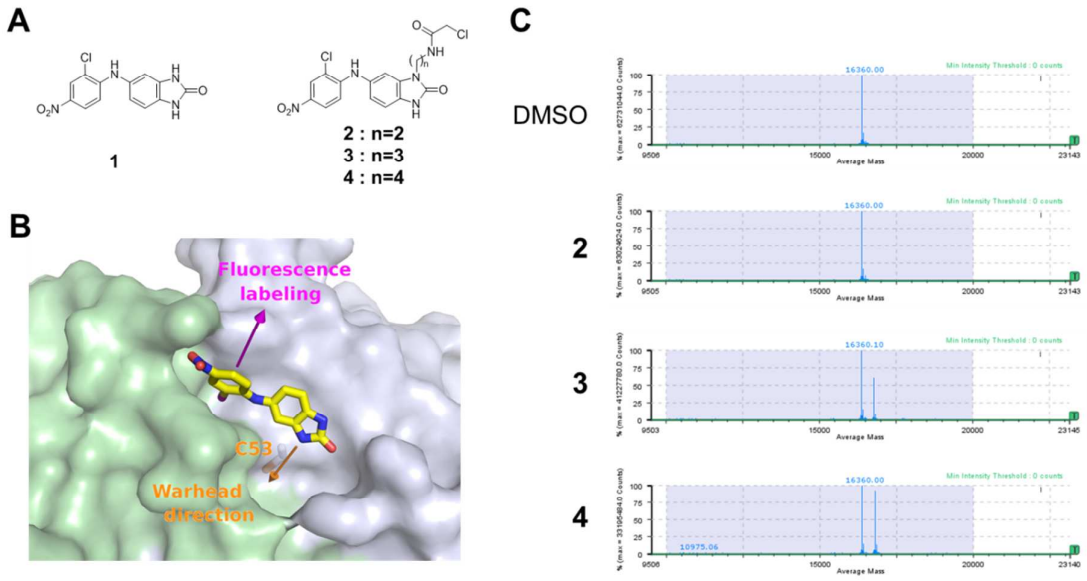

Figure 2. (A) Chemical structures of **1**–**4**. (B) Co-crystal structure of BCL6-BTB (C53/C121) with **1** (PDB code 5X9O).[37] (C) protein-MS analysis of covalent modification of BCL6-BTB (C53/C121) with or without **2**–**4**.

Development of an IPC assay based on TR-FRET

As a metric of potency for reversible inhibitors, the PPI's half-maximum inhibitory concentration (IC_{50}) is utilized as a metric of potency for reversible inhibitors; however, for irreversible inhibitors, the IC_{50} values are not an appropriate metric because they decrease in a time-dependent manner. Therefore, the second-order rate constant of target inactivation, k_{inact}/K_I ($M^{-1}s^{-1}$) should be utilized as an evaluation metric for irreversible inhibitors.[20, 21, 38] Previously, we developed an IPC assay based on endpoint analysis to evaluate the k_{inact}/K_I values in a high-throughput manner using a target-specific irreversible probe.[35] To apply an IPC assay to BCL6, we designed and synthesized a covalent fluorescent probe, **BCL6-FP** (**5**, Figure 3A), which introduced a TAMRA fluorophore to solvent-exposed region of **4** (Figure

2B). The interaction between **BCL6-FP** and Avi-tagged BCL6-BTB (C53/C121) complexed with terbium (Tb) conjugated streptavidin (Tb-SA) was measured using TR-FRET. To investigate the irreversible binding of **BCL6-FP** to BCL6-BTB (C53/C121), we confirmed displacement of **BCL6-FP** from the BCL6 protein by its competitor **27** (Figure S6A), a covalent, but non fluorescent, derivative of **BCL6-FP**. Preformed **BCL6-FP** and BCL6 protein complex were not disrupted by the addition of an 800-fold amount of **27**, which indicated irreversible binding of **BCL6-FP** to BCL6-BTB (C53/C121) (Figure S6B). This shows that **BCL6-FP** is a suitable competition probe for the IPC assay. To determine the $(k_{inact}/K_I)_{probe}$ value of **BCL6-FP**, the time-course change in the TR-FRET signal (Figure 3B) was measured. From the replot analysis, $(k_{inact}/K_I)_{probe}$ was calculated to be $(1.3 \pm 0.03) \times 10^3$ $M^{-1}s^{-1}$ (Figure 3C, error represents SEM of the curve fitting). The half-time of the reaction was 34 min in the presence of 250 nM **BCL6-FP** (Figure 3B). Since a period longer than five times the half-time incubation period is required to occupy more than 97% of the receptor,[35] we selected 4 h as an incubation time for the IPC assay.

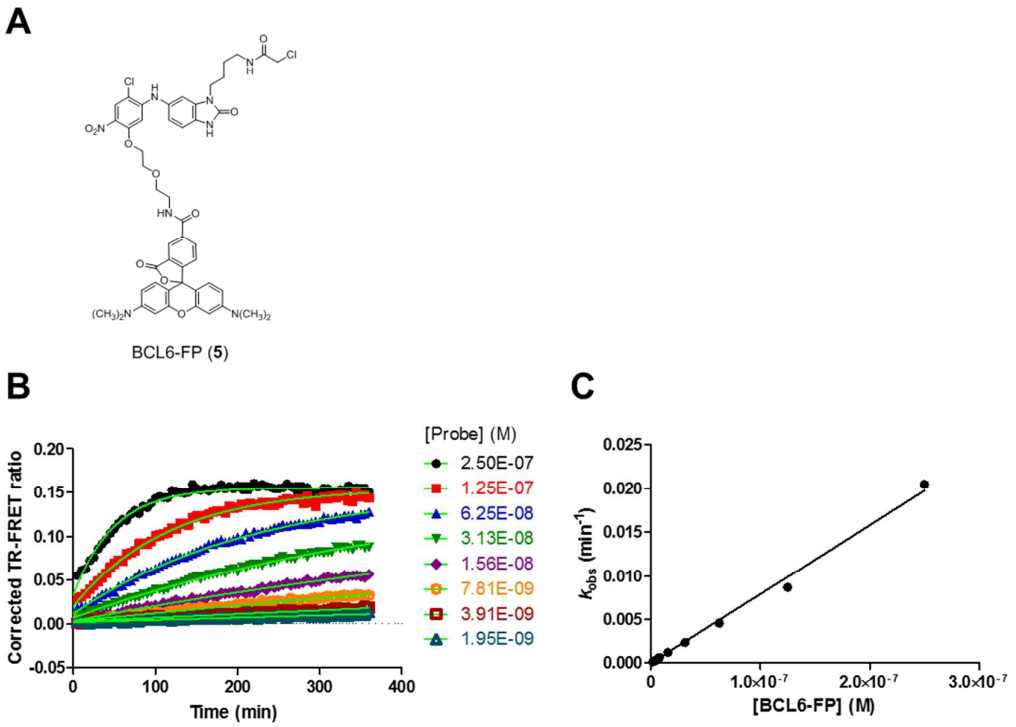

Figure 3. TR-FRET assay development for irreversible BCL6 inhibitors. (A) The chemical structure of **BCL6-FP** (**5**). (B) Corrected TR-FRET time course at varied concentrations of **BCL6-FP**. The target-specific binding TR-FRET signal was obtained by subtracting the signal of the sample without BCL6-BTB (C53/C121) from the signal containing 0.25 nM BCL6. The data are given as the mean ± SEM (n = 4). The solid line is the single exponential curve, $(Y_\infty\text{-}Y_0)[1\text{-}\exp(\text{-}k_{obs})t]+Y_0$, fit to the data by least-squares fitting. (C) Replot of the k_{obs} values versus probe concentration. Data are presented with the SEM from curve fitting. The replot data was fitted with the following equation, $k_{obs} = (k_{inact}/K_I)_{probe}$[**BCL6-FP**].

Irreversible BCL6 inhibitor's chemical optimization based on the k_{inact}/K_I value

Irreversible lead compound **4** was optimized using an IPC assay using the k_{inact}/K_I value as a potency metric. The chemical structures and potencies of the synthesized compounds (**4** and **6**–**8**) are summarized in Figure 4 and Table 1. The k_{inact}/K_I value of **4** was 3.0×10^1 $M^{-1}s^{-1}$. Initially, a 4-tetrahydropyranyloxy moiety (**6**) was introduced to **4** based on our reported structure–activity relationship (SAR) of reversible **1**.[37] As expected, the k_{inact}/K_I

of **6** increased 18-fold compared to that of **4**. We previously found that the benzimidazolone ring could be replaced with the tetrahydroquinolinone ring. Herein, a benzoxazine ring (**7**) was designed based on the direction toward the Cys residue and the synthetic feasibility for a chloroacetamide warhead introduction. This modification led to an additional 7.4-fold increase in potency. Finally, a 2-propanoylaminoethyl moiety (**8**) was introduced to increase the activity. Consequently, **BCL6-i** (**8**) showed 1.9×10^4 $M^{-1}s^{-1}$ in k_{inact}/K_I, corresponding to a 670-fold improvement compared to **4**. Protein-MS analysis showed the covalent binding of **BCL6-i** to BCL6-BTB (C53/C121) with 1:1 stoichiometry (Figure S7). The irreversibility of the interaction between **BCL6-i** and the BCL6 protein was confirmed by a time-dependent IC_{50} change in the IPC assay. As stated in the previous report,[35] irreversibility of the interaction can be investigated by comparison of two IC_{50} values at different time points in the IPC assay. Briefly, irreversible inhibitors produce IC_{50} values that are independent of reaction time, while reversible inhibitors will produce IC_{50} values that weaken with increasing assay time. Comparing IC_{50} values after 4 h and 12 h incubation in an IPC assay, **BCL6-i** showed an identical IC_{50} value (Figure S8A), which indicated irreversible binding of **BCL6-i** with the BCL6-BTB (C53/C121) protein. To confirm a Cys53 specific modification of **BCL6-i**, we examined the time-dependent inhibition of the reversible interaction between BCL6 mutants and the TAMRA-peptide. In the reversible peptide competition assay, **BCL6-i** inhibited BCL6 mutants containing Cys53 (Figure S9A, C, E) in a time-dependent manner.

Conversely, the difference between the IC_{50} values of **BCL6-i** after 10 and 60 min was within 2-fold. (Figure S9B, D, E). This result suggests Cys53 in BCL6-BTB was specifically modified by the optimized **BCL6-i**.

Improvement in the k_{inact}/K_I via increasing the intrinsic chemical reactivity (k_{chem}) of compounds is not desirable because a large k_{chem} correlates with covalent off-target modification, leading to toxicity and adverse side-effects.[27–29] To investigate the cause of k_{inact}/K_I improvement for this inhibitor series, the k_{chem} of the irreversible BCL6 inhibitors **4** and **6**–**8** were measured, and the results are summarized in Table 1. Since all of the compounds possess the same warhead, all irreversible BCL6 inhibitors showed comparable k_{chem} values. In our experimental conditions, these k_{chem} values were smaller than that reported for irreversible kinase inhibitors. Among them, CI-1033 proceeded to clinical trials,[30, 31] which indicated an acceptable intrinsic chemical reactivity of **BCL6-i** for cellular or *in vivo* evaluation.

To evaluate if another chemical warhead can also covalently modify the BCL6 protein, we synthesized **BCL6-NC** (**9**), an acrylamide derivative of **BCL6-i**. Even after overnight incubation, **BCL6-NC** did not show covalent bond formation with BCL6-BTB (C53/C121) (Figure S10A). Additionally, time-dependent inhibition of the reversible interaction between BCL6-BTB (C53/C121) and the TAMRA-peptide was not observed (Figure S10B), which suggested that **BCL6-NC** does not irreversibly inhibit BCL6-BTB

(C53/C121). We further investigated the reversibility of the interaction between **BCL6-NC** and BCL6-BTB (C53/C121) protein using an IPC assay. Unlike **BCL6-i** (Figure S8A), **BCL6-NC** produced IC_{50} values that weakened with increasing assay time (Figure S8B), which indicated reversible binding of **BCL6-NC** to BCL6-BTB (C53/C121).

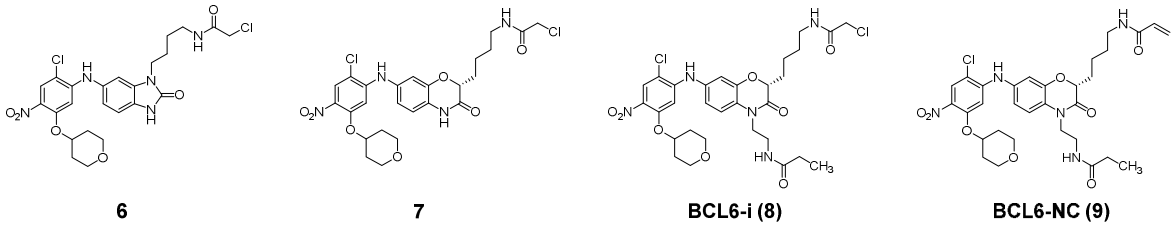

Figure 4. Chemical structure of **6–9**.

Table 1. Irreversible inhibitory activity (k_{inact}/K_I) and intrinsic chemical reactivity (k_{chem}) of the BCL6 inhibitors

Compound	k_{inact}/K_I [a] ($M^{-1}s^{-1}$)	k_{chem} [b] ($M^{-1}s^{-1}$)
4	$(3.0 \pm 0.2)\times10^{1}$	$(8.6 \pm 1.1)\times10^{-4}$
6	$(5.4 \pm 1.9)\times10^{2}$	$(9.6 \pm 1.1)\times10^{-4}$
7	$(4.0 \pm 1.2)\times10^{3}$	$(2.0 \pm 0.09)\times10^{-3}$
BCL6-i (8)	$(1.9 \pm 0.6)\times10^{4}$	$(1.6 \pm 0.02)\times10^{-3}$
CI-1033		$(3.7 \pm 0.05)\times10^{-2}$
WZ-8040		$(7.7 \pm 0.2)\times10^{-3}$

[a] Data represents mean ± SEM of three independent experiments. [b] Error represents the SEM of curve fitting.

Confirmation of BCL6-NC as a negative control for BCL6-i

Since **BCL6-NC** has a similar physicochemical property (molecular weight,

lipophilicity, and membrane permeability) to **BCL6-i** (Table S1), **BCL6-NC** can be utilized as a negative control for **BCL6-i**. To investigate whether **BCL6-NC** can be an appropriate negative control for further experiments, we first confirmed the k_{chem} of **BCL6-NC** because high chemical reactivity leads to promiscuous intracellular protein inhibition.[39, 40] As shown in Figure S11, we could hardly detect the reactivity of **BCL6-NC** in the time period tested, verifying that the k_{chem} of **BCL6-NC** is lower than that of **BCL6-i**. This result indicated that the potential for promiscuous covalent inhibition by **BCL6-NC** is extremely low. To our surprise, compared to the irreversible kinase inhibitors with acrylamide evaluated in this study (Table 1), **BCL6-NC** showed lower thiol reactivity in spite of the presence of the same acrylamide warhead (Figure S11). According to a previous report,[39] k_{chem} of aryl acrylamide is higher than that of alkyl acrylamide, when compared under the same chemical scaffolds. Therefore, the lower reactivity of **BCL6-NC** may derive from the difference of functional groups adjacent to the chemical warhead. To explicit the cause of the k_{chem} difference, however, we may require SAR study for the thiol reactivity of acrylamide warhead by synthesis of analogue compounds of **BCL6-i**, such as phenyl acrylamide.

Since the warhead size of **BCL6-NC** is not equivalent to that of **BCL6-i**, reversible affinity (K_i) of **BCL6-NC** may be considerably different from that of **BCL6-i**. To rule out this possibility, we compared the K_i of these compounds to the BCL6 protein. Since direct measurement of the K_i for **BCL6-i** to BCL6-BTB (C53/C121) was difficult due to its

covalent modification, we utilized a cysteine-free BCL6-BTB mutant (C53S/C121S) as a surrogate protein to measure the affinity of **BCL6-i** and **BCL6-NC**. As shown in Table S2, the K_i of **BCL6-i** and **BCL6-NC** to BCL6-BTB (C53S/C121S) was almost equivalent. The K_i value of **BCL6-NC** for BCL6-BTB (C53S/C121S) was similar to that for BCL6-BTB (C53/C121), which suggested the affinity of these compounds can be appropriately evaluated using the cysteine-free mutant. Taken together, **BCL6-NC** possesses the similar binding affinity to **BCL6-i** but does not covalently bind to BCL6-BTB (C53/C121), suggesting that **BCL6-NC** can be used as a negative control for **BCL6-i**.

Confirmation of intracellular target engagement of irreversible BCL6-i by fluorescence imaging

To assess the irreversible binding of **BCL6-i** to the intracellular BCL6 protein, we analyzed co-localization of **BCL6-FP** with the BCL6 protein using fluorescence imaging. **BCL6-FP** was added to U2OS cells expressing FLAG-BCL6 (wild type, full length), and the cells were fixed for immunostaining using an Alexa488-conjugated anti-FLAG antibody. Even after fixation and washing, the co-localization of **BCL6-FP** with the BCL6 protein was observed (Figure 5, *top*), which suggested **BCL6-FP** irreversibly interacts with the intracellular BCL6 protein.

Next, we examined if **BCL6-i** interacts with intracellular BCL6 by monitoring the

displacement of **BCL6-FP**. **BCL6-i** decreased the fluorescence signal of **BCL6-FP** to the base levels (Figure 5, *middle*), whereas **BCL6-NC** did not (Figure 5, *bottom*). These results suggested that **BCL6-i** was irreversibly bound to intracellular BCL6 in a physiological environment.

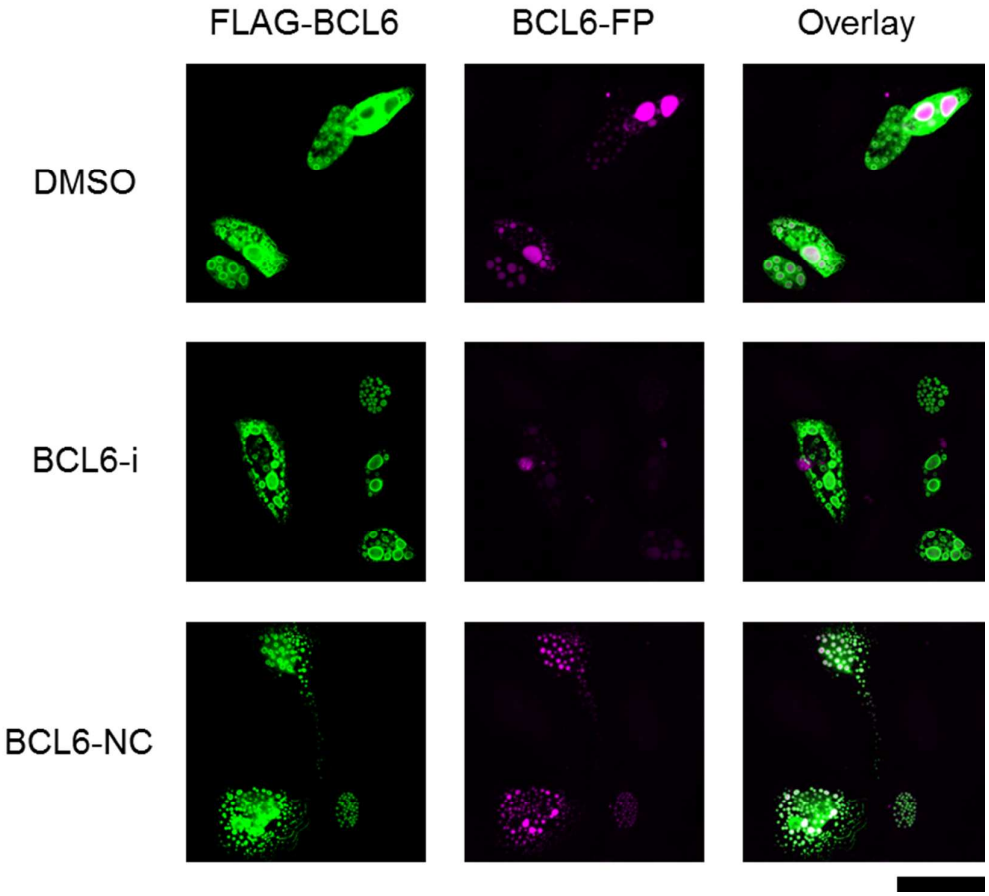

Figure 5. Target engagement of the BCL6 inhibitor using fluorescence imaging. U2OS cells expressing FLAG-BCL6 (wild type, full length) were treated with DMSO (*top*), 1 μM **BCL6-i** (*middle*), and 1 μM **BCL6-NC** (*bottom*) for 1 h, followed by reaction with 1 μM **BCL6-FP** for 1 h. Co-localization of BCL6 (*green*) and BCL6-FP (*magenta*) was visualized using an INCell Analyzer 6000. The scale bar represents 50 μm.

Confirmation of intracellular BCL6/BCOR interaction inhibition by BCL6-i using a M2H assay

To confirm if irreversible binding of **BCL6-i** to BCL6 lead to inhibition of the PPI between intracellular BCL6 and its corepressors, we performed an M2H assay. GAL4-BCL6 (Ala5–Glu129) and VP16-BCOR (Leu112–Ala753) were co-expressed in HEK293T cells and the M2H signal was observed after a 24 h inhibitor treatment. **BCL6-i** significantly inhibited the M2H signal derived from the BCL6/BCOR interaction, whereas the negative control compound **BCL6-NC** did not (Figure 6). This suggested that **BCL6-i** inhibited the intracellular BCL6/BCOR interaction.

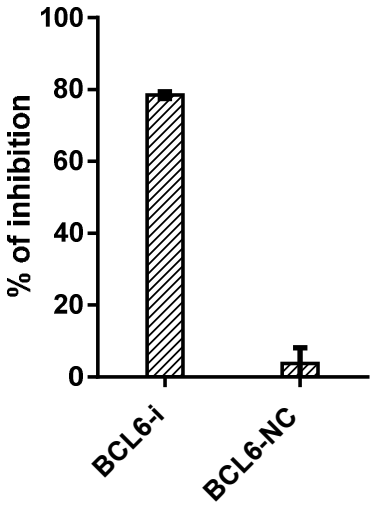

Figure 6. M2H analysis of BCL6/BCOR inhibition using 1 μM **BCL6-i** and 1 μM **BCL6-NC**. Error bar represents SEM (n = 4).

Confirmation of BCL6-dependent cell-line growth inhibition by BCL6-i

Finally, we investigated cell-growth suppression via inhibition by **BCL6-i**. BCL6-dependent DLBCL cell lines (SUDHL4 and OCI-LY3)[18] were treated with **BCL6-i** or **BCL6-NC** for 3 days; thereafter, the viability was measured. **BCL6-i** significantly

suppressed the DLBCL cell-line growth compared to **BCL6-NC** (Figure 7). The reason for growth inhibition of these cell lines by **BCL6-i** is inhibition of the intracellular PPI between BCL6 and its corepressors (Figure 5 and 6).

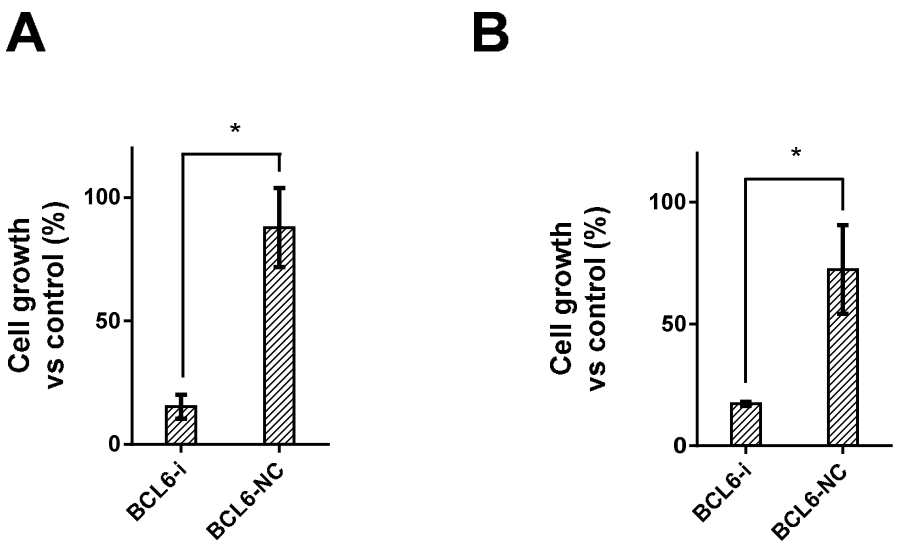

Figure 7. GCB-DLBCL cell-growth inhibition by **BCL6-i** and **BCL6-NC**. GCB-DLBCL cells ((A) SUDHL4 and (B) OCI-LY3) were treated with 3 μM of the test compounds and the viability was measured after a 3-day incubation. Data represents mean ± SD (n = 4). (*$p < 0.001$, Student's *t*-test)

DISCUSSIONS

In this study, we successfully developed a potent, cell-active, BCL6 inhibitor: **BCL6-i**. The optimization process for the irreversible inhibitor presented herein can be regarded as a widely applicable approach for drug discovery. Once an irreversible lead inhibitor is identified, an irreversible fluorescent probe can be prepared based on the lead compound. Through the use of an irreversible fluorescent probe, chemical optimization can be performed by SAR studies based on k_{inact}/K_I values using an IPC assay. After chemical

optimization, the intracellular target engagement of the test compound can be confirmed using the irreversible fluorescent probe. Target-engagement evaluation using this approach will contribute to the understanding of the physiological phenomena induced by the compound.

Herein, we designed an irreversible BCL6 inhibitor, **BCL6-i**, targeting Cys53 located at the protein–protein interaction interface. We confirmed the covalent binding of BCL6-i using MS analysis with 1:1 binding stoichiometry (Figure S7), indicating that **BCL6-i** covalently binds to either Cys53 or Cys121 of BCL6-BTB protein. To clarify the covalent binding to Cys53, time-dependent binding of **BCL6-i** to BCL6-BTB mutants was evaluated in protein-peptide interaction (PPI) assay using reversible fluorescence peptide (Figure S9). **BCL6-i** exhibited time-dependent inhibition only to mutants containing Cys53 of BCL6-BTB, suggesting the covalent binding to Cys53, not to Cys121. Although these results strongly indicates specific covalent modification of Cys53, the possibility that **BCL6-i** also covalently modifies Cys121 is still remaining since we have not directly confirmed covalent bond formation between **BCL6-i** and Cys53 of BCL6. To obtain more direct evidence of specific covalent modification of Cys53 by **BCL6-i**, we have tried X-ray crystal structural analysis of BCL6 protein and **BCL6-i** (and their analogues) complex. Although extra electron density around Cys53 has been obtained in low resolution, the data still need to be refined (data not shown). To definitively demonstrate the Cys53 specific modification,

additional experiment is required, such as MS analysis of **BCL6-i** adduct to BCL6 mutants (C53/C53S and C53S/C121) or identification of modification site using protease digestion followed by MS/MS analysis.

We demonstrated that the k_{inact}/K_I value for irreversible inhibitors can be optimized without increasing the intrinsic chemical reactivity. Considering the definition of k_{inact}/K_I ($K_I = (k_{off} + k_{inact})/k_{on}$), the reason for the increase in irreversible BCL6 inhibitor potency is assumed to originate from two factors: The first factor is improvement of the reversible interaction ($K_i = k_{off}/k_{on}$) between BCL6 and the compounds; K_i might increase by structural optimization of the linker and the warhead (alkyl chloroacetamide moiety).[37] The second factor is an increase in the k_{inact} value. Improvement of k_{inact} is considered to be caused by the following two reasons: First, an increase in the intrinsic chemical reactivity (k_{chem}). Although the k_{inact} improvement is easily achieved by k_{chem} enhancement,[25] compounds with a high k_{chem} are not suitable for chemical probes and therapeutic drugs because of potential promiscuous protein modification, which leads to off-target inhibition and adverse side-effects.[27–29] Second, for k_{inact} improvement, optimization of the distance between the covalent warhead and the target residue can be performed. We confirmed that the k_{chem} value did not change in the chemical optimization process (Table 1). Since the k_{chem} of **BCL6-i** was smaller than that of CI-1033, an irreversible inhibitor currently under clinical trial tests (Table 1),[30, 31] the intrinsic chemical reactivity of **BCL6-i** is expected to be acceptable for cellular or

in vivo testing. To optimize selective irreversible inhibitors, the k_{inact}/K_I should be improved without a k_{chem} increase. For this reason, simultaneous evaluation of k_{inact}/K_I and k_{chem} (a two dimensional SAR study) is widely recommended for designing target-specific irreversible inhibitors.

Herein, we showed the advantage of using irreversible inhibition for identification of PPI inhibitors. PPI is considered a challenging drug target class for small-molecule potent-inhibitor identification because of the lack of deep cavities on the interaction surface.[14–17] Theoretically, irreversible inhibitors can occupy all target-protein molecules after a sufficient incubation time, and are expected to exert potent pharmacological efficacy until the next turnover of the protein.[35] Despite the desirable features, irreversible inhibitors have been avoided in drug-discovery programs for several decades due to their potential for promiscuous target inhibition.[27–29] As shown herein, two dimensional SAR studies of k_{inact}/K_I and k_{chem} will contribute to the discovery of potent irreversible inhibitors with low intrinsic chemical reactivity. As long as a targetable cysteine residue is present in the interface of a PPI, irreversible inhibition should be considered for identifying potent inhibitors and chemical probes.

In this study, the irreversible fluorescence probe **BCL6-FP** was utilized for k_{inact}/K_I evaluation using an IPC assay and the confirmation of intracellular target engagement of the compounds. Confirmation of intracellular target engagement is extremely important for

determining if the efficacy in cellular assays is derived from the intended target.[41, 42] Additionally, confirmation of target occupancy is necessary for extrapolation of *in vitro* assay results to *in vivo* efficacy.[43] Unlike reversible inhibitors, irreversible inhibitors maintain target-protein occupation after lowering the pharmacological concentrations of the drug in systemic circulation, thus leading to a prolonged pharmacological effect *in vivo*.[20, 22, 43] To predict or interpret *in vivo* pharmacodynamics marker changes from irreversible inhibitors, pharmacokinetic analysis alone is not sufficient and a time-course measurement of target occupancy should be performed after drug administration. The advantage of an irreversible covalent probe is that it allows easy intracellular target-engagement confirmation because the probe still binds to the protein via a covalent bond even under harsh conditions, such as protein denaturation and cell lysis. Due to the assay convenience, we easily confirmed intracellular target engagement by measuring co-localization of BCL6 and **BCL6-FP** using fluorescence imaging. Theoretically, **BCL6-FP** can be applied to evaluate target occupancy analysis *in vivo*.[44–46] Since a high dose administration of irreversible inhibitors might cause off-target modification, it is important to determine the minimum required dosage to occupy the target and exert drug efficacy. Therefore, target occupancy analysis *in vivo* should be considered for determining the regimen of irreversible inhibitors for *in vivo* testing.

In conclusion, we discovered a cell-active, potent, irreversible BCL6 inhibitor, **BCL6-i**, with an acceptable intrinsic chemical reactivity through the use of an IPC assay.

BCL6-i can be used as a chemical tool to investigate the function of the BCL6 protein and can be further optimized for *in vivo* effective BCL6 inhibitors aimed at novel therapeutic agents for B-cell lymphomas.

ACKNOWLEDGMENTS

We thank Shoichi Okubo for plasmid preparation and Takeshi Yasui for providing information about the SAR of BCL6 inhibitors. The authors thank Seiji Yamasaki for measuring the intrinsic chemical reactivity of compounds using HPLC. We are grateful to Shin-ichi Niwa for parallel artificial membrane permeability assay (PAMPA) experiment. The authors thank Junji Matsui for encouraging this research. The authors also thank Enago (www.enago.jp) for the English language review.

Competing Interests

The authors declare that there are no competing interests associated with the manuscript.

Funding Information

This research did not receive any specific grant from funding agencies in the public, commercial, or not-for-profit sectors.

Present Address

[§]For K.S.: Ichimaru Pharcos Company Limited, 318-1 Asagi, Motosu-shi, Gifu 501-0475, Japan.

Author contribution

T.S. and I.M. designed the experiments; T.Y. designed and synthesized the irreversible BCL6 inhibitors, T.S. and M.G. performed the TR-FRET experiments; S.I. conducted protein-MS analysis; O.S. performed fluorescence imaging and growth inhibition test; K.S. designed the M2H assay and the assay was performed by K.S. and T.S.; K.S. identified the BCL6 inhibiting peptide using phage display technology; K.I. prepared BCL6 mutant proteins; S. S. analyzed crystal structure of BCL6 complexed with a fragment compound. T.S. analyzed the experimental data; T.S., T.Y., O.S., S.S., Y.I., J.S., and I. M. jointly wrote the paper. All authors have read and approved the final manuscript.

Supporting Information

Supporting assay methods and results. Synthesis methods for compounds utilized in this study.

■ REFERENCES

1. Stogios, P. J., Downs, G. S., Jauhal, J. J., Nandra, S. K., and Prive, G. G. (2005) Sequence and structural analysis of BTB domain proteins, *Genome Biol. 6*, R82.
2. Basso, K., and Dalla-Favera, R. (2012) Roles of BCL6 in normal and transformed germinal center B cells, *Immunol. Rev. 247*, 172–183.
3. Ye, B. H. (2000) BCL-6 in the pathogenesis of non-Hodgkin's lymphoma, *Cancer Invest. 18*, 356–365.
4. Cattoretti, G., Chang, C. C., Cechova, K., Zhang, J., Ye, B. H., Falini, B., Louie, D. C., Offit, K., Chaganti, R. S., and Dalla-Favera, R. (1995) BCL-6 protein is expressed in germinal-center B cells, *Blood 86*, 45–53.
5. Dhordain, P., Albagli, O., Lin, R. J., Ansieau, S., Quief, S., Leutz, A., Kerckaert, J. P., Evans, R. M., and Leprince, D. (1997) Corepressor SMRT binds the BTB/POZ repressing domain of the LAZ3/BCL6 oncoprotein, *Proc. Natl. Acad. Sci. U. S. A. 94*, 10762–10767.
6. Huynh, K. D., and Bardwell, V. J. (1998) The BCL-6 POZ domain and other POZ domains interact with the co-repressors N-CoR and SMRT, *Oncogene 17*, 2473–2484.
7. Huynh, K. D., Fischle, W., Verdin, E., and Bardwell, V. J. (2000) BCoR, a novel corepressor involved in BCL-6 repression, *Genes Dev. 14*, 1810–1823.
8. Ghetu, A. F., Corcoran, C. M., Cerchietti, L., Bardwell, V. J., Melnick, A., and Prive, G. G. (2008) Structure of a BCOR corepressor peptide in complex with the BCL6 BTB domain dimer, *Mol. Cell 29*, 384–391.
9. Ahmad, K. F., Melnick, A., Lax, S., Bouchard, D., Liu, J., Kiang, C. L., Mayer, S., Takahashi, S., Licht, J. D., and Prive, G. G. (2003) Mechanism of SMRT corepressor recruitment by the BCL6 BTB domain, *Mol. Cell 12*, 1551–1564.
10. Polo, J. M., Dell'Oso, T., Ranuncolo, S. M., Cerchietti, L., Beck, D., Da Silva, G. F., Prive, G. G., Licht, J. D., and Melnick, A. (2004) Specific peptide interference reveals BCL6 transcriptional and oncogenic mechanisms in B-cell lymphoma cells, *Nat. Med. 10*, 1329–1335.
11. Cerchietti, L. C., Yang, S. N., Shaknovich, R., Hatzi, K., Polo, J. M., Chadburn, A., Dowdy, S. F., and Melnick, A. (2009) A peptomimetic inhibitor of BCL6 with potent antilymphoma effects in vitro and in vivo, *Blood 113*, 3397–3405.
12. Polo, J. M., Juszczynski, P., Monti, S., Cerchietti, L., Ye, K., Greally, J. M., Shipp, M., and Melnick, A. (2007) Transcriptional signature with differential expression of BCL6 target genes accurately identifies BCL6-dependent diffuse large B cell lymphomas, *Proc. Natl. Acad. Sci. U. S. A. 104*, 3207–3212.
13. Wagner, S. D., Ahearne, M., and Ko Ferrigno, P. (2011) The role of BCL6 in lymphomas and routes to therapy, *Br. J. Haematol. 152*, 3–12.
14. Sameshima, T., Miyahisa, I., Homma, M., Aikawa, K., Hixon, M. S., and Matsui, J. (2014) A simple and widely applicable hit validation strategy for protein-protein interaction inhibitors based

on a quantitative ligand displacement assay, *Bioorg. Med. Chem. Lett. 24*, 5836–5839.

15. Mullard, A. (2012) Protein-protein interaction inhibitors get into the groove, *Nat. Rev. Drug Discov. 11*, 173–175.
16. Arkin, M. R., and Wells, J. A. (2004) Small-molecule inhibitors of protein-protein interactions: progressing towards the dream, *Nat. Rev. Drug Discov. 3*, 301–317.
17. Wells, J. A., and McClendon, C. L. (2007) Reaching for high-hanging fruit in drug discovery at protein-protein interfaces, *Nature 450*, 1001–1009.
18. Cardenas, M. G., Yu, W., Beguelin, W., Teater, M. R., Geng, H., Goldstein, R. L., Oswald, E., Hatzi, K., Yang, S. N., Cohen, J., Shaknovich, R., Vanommeslaeghe, K., Cheng, H., Liang, D., Cho, H. J., Abbott, J., Tam, W., Du, W., Leonard, J. P., Elemento, O., Cerchietti, L., Cierpicki, T., Xue, F., MacKerell, A. D., Jr., and Melnick, A. M. (2016) Rationally designed BCL6 inhibitors target activated B cell diffuse large B cell lymphoma, *J. Clin. Invest. 126*, 3351–3362.
19. Cerchietti, L. C., Ghetu, A. F., Zhu, X., Da Silva, G. F., Zhong, S., Matthews, M., Bunting, K. L., Polo, J. M., Fares, C., Arrowsmith, C. H., Yang, S. N., Garcia, M., Coop, A., Mackerell, A. D., Jr., Prive, G. G., and Melnick, A. (2010) A small-molecule inhibitor of BCL6 kills DLBCL cells in vitro and in vivo, *Cancer Cell 17*, 400–411.
20. Strelow, J. M. (2017) A Perspective on the Kinetics of Covalent and Irreversible Inhibition, *SLAS Discov. 22*, 3–20.
21. Singh, J., Petter, R. C., Baillie, T. A., and Whitty, A. (2011) The resurgence of covalent drugs, *Nat. Rev. Drug Discov. 10*, 307–317.
22. Barf, T., and Kaptein, A. (2012) Irreversible protein kinase inhibitors: balancing the benefits and risks, *J. Med. Chem. 55*, 6243–6262.
23. Bauer, R. A. (2015) Covalent inhibitors in drug discovery: from accidental discoveries to avoided liabilities and designed therapies, *Drug Discov. Today 20*, 1061–1073.
24. Akcay, G., Belmonte, M. A., Aquila, B., Chuaqui, C., Hird, A. W., Lamb, M. L., Rawlins, P. B., Su, N., Tentarelli, S., Grimster, N. P., and Su, Q. (2016) Inhibition of Mcl-1 through covalent modification of a noncatalytic lysine side chain, *Nat. Chem. Biol. 12*, 931–936.
25. Schwartz, P. A., Kuzmic, P., Solowiej, J., Bergqvist, S., Bolanos, B., Almaden, C., Nagata, A., Ryan, K., Feng, J., Dalvie, D., Kath, J. C., Xu, M., Wani, R., and Murray, B. W. (2014) Covalent EGFR inhibitor analysis reveals importance of reversible interactions to potency and mechanisms of drug resistance, *Proc. Natl. Acad. Sci. U. S. A. 111*, 173–178.
26. Liu, Q., Sabnis, Y., Zhao, Z., Zhang, T., Buhrlage, S. J., Jones, L. H., and Gray, N. S. (2013) Developing irreversible inhibitors of the protein kinase cysteinome, *Chem. Biol. 20*, 146-159.
27. Potashman, M. H., and Duggan, M. E. (2009) Covalent modifiers: an orthogonal approach to drug design, *J. Med. Chem. 52*, 1231–1246.
28. Uetrecht, J. (2009) Immune-mediated adverse drug reactions, *Chem. Res. Toxicol. 22*, 24–34.
29. Johnson, D. S., Weerapana, E., and Cravatt, B. F. (2010) Strategies for discovering and derisking covalent, irreversible enzyme inhibitors, *Future Med. Chem. 2*, 949–964.

30. Janne, P. A., von Pawel, J., Cohen, R. B., Crino, L., Butts, C. A., Olson, S. S., Eiseman, I. A., Chiappori, A. A., Yeap, B. Y., Lenehan, P. F., Dasse, K., Sheeran, M., and Bonomi, P. D. (2007) Multicenter, randomized, phase II trial of CI-1033, an irreversible pan-ERBB inhibitor, for previously treated advanced non small-cell lung cancer, *J. Clin. Oncol. 25*, 3936–3944.

31. Campos, S., Hamid, O., Seiden, M. V., Oza, A., Plante, M., Potkul, R. K., Lenehan, P. F., Kaldjian, E. P., Varterasian, M. L., Jordan, C., Charbonneau, C., and Hirte, H. (2005) Multicenter, randomized phase II trial of oral CI-1033 for previously treated advanced ovarian cancer, *J. Clin. Oncol. 23*, 5597–5604.

32. Zhou, W., Ercan, D., Chen, L., Yun, C. H., Li, D., Capelletti, M., Cortot, A. B., Chirieac, L., Iacob, R. E., Padera, R., Engen, J. R., Wong, K. K., Eck, M. J., Gray, N. S., and Janne, P. A. (2009) Novel mutant-selective EGFR kinase inhibitors against EGFR T790M, *Nature 462*, 1070–1074.

33. Chen, I., Howarth, M., Lin, W., and Ting, A. Y. (2005) Site-specific labeling of cell surface proteins with biophysical probes using biotin ligase, *Nature Method. 2*, 99–104.

34. Sakamoto, K., Sogabe, S., Kamada, Y., Sakai, N., Asano, K., Yoshimatsu, M., Ida, K., Imaeda, Y., and Sakamoto, J. I. (2017) Discovery of high-affinity BCL6-binding peptide and its structure-activity relationship, *Biochem. Biophys. Res. Commun. 482*, 310–316.

35. Miyahisa, I., Sameshima, T., and Hixon, M. S. (2015) Rapid Determination of the Specificity Constant of Irreversible Inhibitors (kinact/KI) by Means of an Endpoint Competition Assay, *Angew. Chem. Int. Ed. 54*, 14099–14102.

36. Sameshima, T., Tanaka, Y., and Miyahisa, I. (2017) Universal and Quantitative Method To Evaluate Inhibitor Potency for Cysteinome Proteins Using a Nonspecific Activity-Based Protein Profiling Probe, *Biochemistry 56*, 2921–2927.

37. Yasui, T., Yamamoto, T., Sakai, N., Asano, K., Takai, T., Yoshitomi, Y., Davis, M., Takagi, T., Sakamoto, K., Sogabe, S., Kamada, Y., Lane, W., Snell, G., Iwata, M., Goto, M., Inooka, H., Sakamoto, J. I., Nakada, Y., and Imaeda, Y. (2017) Discovery of a novel B-cell lymphoma 6 (BCL6)-corepressor interaction inhibitor by utilizing structure-based drug design, *Bioorg. Med. Chem. 25*, 4876–4886.

38. Copeland, R. A. (2005) Irreversible Enzyme Inactivators. In Evaluation of enzyme inhibitors in drug discovery. A guide for medicinal chemists and pharmacologists., 214–248, Wiley, Hoboken.

39. Flanagan, M. E., Abramite, J. A., Anderson, D. P., Aulabaugh, A., Dahal, U. P., Gilbert, A. M., Li, C., Montgomery, J., Oppenheimer, S. R., Ryder, T., Schuff, B. P., Uccello, D. P., Walker, G. S., Wu, Y., Brown, M. F., Chen, J. M., Hayward, M. M., Noe, M. C., Obach, R. S., Philippe, L., Shanmugasundaram, V., Shapiro, M. J., Starr, J., Stroh, J., and Che, Y. (2014) Chemical and computational methods for the characterization of covalent reactive groups for the prospective design of irreversible inhibitors, *J. Med. Chem. 57*, 10072–10079.

40. Sameshima, T., Miyahisa, I., Yamasaki, S., Gotou, M., Kobayashi, T., and Sakamoto, J. (2017) High-Throughput Quantitative Intrinsic Thiol Reactivity Evaluation Using a Fluorescence-Based Competitive Endpoint Assay, *SLAS Discov.*, doi: 10.1177/247255521770465

41. Dubach, J. M., Kim, E., Yang, K., Cuccarese, M., Giedt, R. J., Meimetis, L. G., Vinegoni, C., and Weissleder, R. (2017) Quantitating drug-target engagement in single cells in vitro and in vivo, *Nat. Chem. Biol. 13*, 168–173.

42. Martinez Molina, D., Jafari, R., Ignatushchenko, M., Seki, T., Larsson, E. A., Dan, C., Sreekumar, L., Cao, Y., and Nordlund, P. (2013) Monitoring drug target engagement in cells and tissues using the cellular thermal shift assay, *Science 341*, 84–87.

43. Daryaee, F., Zhang, Z., Gogarty, K. R., Li, Y., Merino, J., Fisher, S. L., and Tonge, P. J. (2017) A quantitative mechanistic PK/PD model directly connects Btk target engagement and in vivo efficacy, *Chem. Sci. 8*, 3434–3443.

44. Honigberg, L. A., Smith, A. M., Sirisawad, M., Verner, E., Loury, D., Chang, B., Li, S., Pan, Z., Thamm, D. H., Miller, R. A., and Buggy, J. J. (2010) The Bruton tyrosine kinase inhibitor PCI-32765 blocks B-cell activation and is efficacious in models of autoimmune disease and B-cell malignancy, *Proc. Natl. Acad. Sci. U. S. A. 107*, 13075–13080.

45. Hagel, M., Niu, D., St Martin, T., Sheets, M. P., Qiao, L., Bernard, H., Karp, R. M., Zhu, Z., Labenski, M. T., Chaturvedi, P., Nacht, M., Westlin, W. F., Petter, R. C., and Singh, J. (2011) Selective irreversible inhibition of a protease by targeting a noncatalytic cysteine, *Nat. Chem. Biol. 7*, 22–24.

46. Evans, E. K., Tester, R., Aslanian, S., Karp, R., Sheets, M., Labenski, M. T., Witowski, S. R., Lounsbury, H., Chaturvedi, P., Mazdiyasni, H., Zhu, Z., Nacht, M., Freed, M. I., Petter, R. C., Dubrovskiy, A., Singh, J., and Westlin, W. F. (2013) Inhibition of Btk with CC-292 provides early pharmacodynamic assessment of activity in mice and humans, *J. Pharmacol. Exp. Ther. 346*, 219–228.

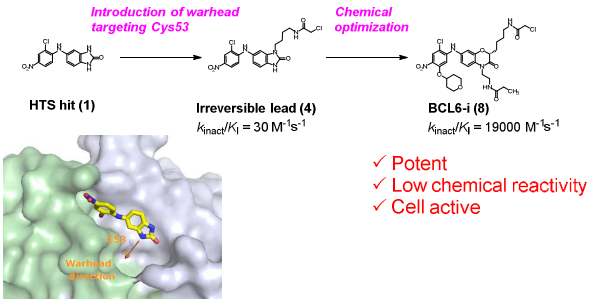

Graphical Table of Contents